

A
Thesis
On
**“TESTING OF PROXIMITY POTENTIALS IN
DIFFERENT MASS REGIONS”**

Submitted in the fulfilment of the partial requirements for the award of
degree of

Master of Science

In
Physics
(2015-2017)

Submitted by

Arpita
(301504008)

Under the guidance of

Dr. Raj Kumar
(Assistant Professor)



SCHOOL OF PHYSICS AND MATERIALS SCIENCE

THAPAR UNIVERSITY

PATIALA – 147004

July 2017

A grateful heart is a beginning of greatness

I dedicate this thesis to my parents *RAMESH CHAND MEHLA* and *RAJ RANI MEHLA*. I am really thankful for providing me the best education and inspiring me so that i can accomplish my dreams.

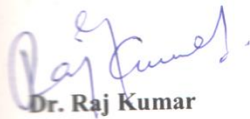
CERTIFICATE

This is to certify that this Thesis entitled “**Testing of Proximity potentials in different mass regions**” is submitted by **Ms. Arpita** (Roll. No. 301504008) in the fulfilment of the partial requirement for the award of degree of Master in Science in **Physics** from School of Physics and Materials Science, Thapar University, Patiala (Punjab), India. It is an exclusive record of candidate’s own research under the supervision of **Dr. Raj Kumar**. This Thesis in part or full has not been submitted in any other institute for award of such kind of degree.


Arpita

(301504008)

Date: 17/07/2017


Dr. Raj Kumar

(Assistant Professor)

School of Physics and Materials Science

Thapar University, Patiala-147004

ACKNOWLEDGMENT

I am submitting my Thesis for the fulfilment of my 'M.Sc.' degree. This work would not have been accomplished without the help, support and guidance of a large number of people. I express my deep gratitude and respect to my supervisor **Dr. Raj Kumar** (Assistant Professor, School of Physics and Materials Science) for his strong motivation, trust and constant encouragement during the course of work. I thank him for his great patience, constructive criticism and for giving me the opportunity to undertake this project.

I also express my heartiest gratitude to **Dr. Manoj Kumar Sharma** (Head and Professor, School of Physics and Material Science) for his support throughout the period and all the members of School of Physics and Materials Science for their help and suggestions at different stages of this work.

The meaning of my life and work is incomplete without paying regards to my respected family whose blessings and continuous encouragement have shown me the path to achieve my goals.

My special thanks to **Ms. Rajni Mittal, Ms. Ishita Sharma** and **Mrs. Navjot Kaur Virk**, Research scholars for their moral support, patience, love and kindness to finish this work. Thanks are also due to all the research scholar of nuclear physics lab for their timely help.

Last but not the least I express my love and respect to my brothers **Mr. Swapan Mehla** and **Mr. Sanyam Mehla** and my friends for their support, motivation, trust and constant co-operation whenever I required.

And above all, I pay my regards to the Almighty for his blessings.

Arpita

LIST OF FIGURES / TABLES

Figure	Title	Page No.
Figure 1.1	Total interaction potential shown for $^{19}\text{F}+^{139}\text{La}$ reaction as a function of internuclear separation.	4
Figure 1.2	Multipole deformations along with their shapes	7
Figure 1.3	The deformation of the colliding nuclei on collision axis for both cold and hot configuration.	8
Figure 3.1	Total interaction potential calculated V (MeV) as a function of radius R (fm) for $^{16}\text{O}+^{176}\text{Yb}$ reaction using Prox 77, Prox 88, Bass 80, BW 91, CW 76 potentials at $T=0$ for (a) the spherical and (b) deformed choice of nuclei along with the optimum orientations..	22
Figure 3.2	Fusion excitation function using various proximity potential for the reactions (a) $^{28}\text{Si} + ^{28}\text{Si}$, (b) $^{74}\text{Ge} + ^{74}\text{Ge}$, (c) $^{16}\text{O} + ^{176}\text{Yb}$ and (d) $^{27}\text{Al} + ^{238}\text{U}$ calculated with the Wong formula considering spherical choice of nuclei and compared with the available experimental data.	23
Figure 3.3	Same as Fig. 3.2 but for deformed choice of nuclei.	26
Figure 3.4	Fusion excitation function using various proximity potential for the reactions (a) $^{28}\text{Si} + ^{30}\text{Si}$, (b) $^{130}\text{Te}+^{64}\text{Ni}$, (c) $^{19}\text{F} + ^{139}\text{La}$ and (d) $^{35}\text{Cl}+ ^{238}\text{U}$ calculated with the Wong formula considering spherical choice of nuclei and compared with the experimental data.	29
Figure 3.5	Same as Fig. 3.4 but for deformed choice of nuclei.	30

Abstract

The present work deals with the proximity potential which is an important aspect for the study of nuclear interaction. Various types of proximity potential have been investigated over the years. In our present work, we choose five such potentials as they cover wide barrier characteristics. These potentials are studied in the different mass regions for the fusion cross section using Wong formula to check their effectiveness. This thesis comprises of three chapters. A brief account of each is described below.

Chapter-1 consist of introductory part of nuclear reaction, low energy heavy –ion reaction, nucleus-nucleus interaction potential and the proximity formalism. To study the effect of nuclear potential the mass regions are described. Beside this, the role of deformation and orientation has been discussed.

Chapter-2 give the details of the methodology used. In this chapter, firstly various proximity potentials are explained. Further, Wong model is described which is used to calculate the fusion cross section.

Chapter-3 presents the calculation and results. The interaction potential is calculated using five nuclear proximity potentials for spherical choice of nuclei and then effect of deformation and orientations is shown on these potentials. Afterwards, fusion excitation functions are calculated for two sets of reactions from four different mass regions of the periodic table, as defined in Chapter 1, with and without the effect of deformation and orientation in order to investigate that which nuclear potential works well in the considered mass regions.

Table of Contents

Chapter -1

1.1	Introduction	1
1.2	Nuclear Reactions	2
1.3	Low Energy heavy ion reactions	3
1.4	Nucleus- nucleus interaction potential	4
1.5	Proximity formalism	5
1.6	Different mass regions	6
1.7	Effect of deformation and orientation	7
	References	11

Chapter-2

2.1	Total interaction potential	13
2.1.1	Coulomb potential	13
2.1.2	Angular momentum dependent potential	14
2.1.3	Proximity potential for deformed and oriented nuclei.	14
2.2	Wong Formula	17
	References	19

Chapter-3

3.1	Introduction	20
3.2	Interaction potential using different proximity potentials.	21
3.3	Fusion cross section in different mass regions of periodic table using various proximity potentials.	22
	References	33
	Summary	34

1.1 Introduction

Nuclear physics is a branch of physics that deals with the study of atomic nuclei, its behavior, structure and its components. Nuclei are studied in a variety of applied pure research but nuclear physics overlaps with members of other fields. It has wide variety of applications which comprises nuclear power, nuclear weapons, nuclear medicines, materials engineering, industrial and agricultural isotopes etc., for better understanding of origin of universe and inner working of stars, its main application i.e. nuclear astrophysics is essential.

In earlier discoveries, the radioactivity was observed by Henry Becquerel in 1896, to understand the structure of atom and nucleus. Later on three types of radiation were discovered by physicists and were named alpha, beta and gamma. Sir J. J. Thomson [1] in his “plum pudding model” describes the inner structure of atom and proposed that atom was considered to be a positively charged ball with negatively charged electrons inserted in it. Later on, Bohr-Rutherford proposed a model, according to which each atom at its center contains an extremely dense, positively charged nucleus which is made up of nucleons (neutrons and protons). Afterwards, Chadwick measured the radii of few heavy nuclei which were found to be much smaller than atomic radii. The issues regarding the structure of the nuclei and its properties were solved by experimental methods proposed by many physicists. Finally, the present understanding of nucleus and atom is a result of efforts made experimentally and theoretically.

The occurrence of various phenomenon like, fusion process inside the sun, working of stars are due to various nuclear reactions. A wide knowledge of nuclear reactions are required to study these processes. To understand the nuclear reaction dynamics various techniques have been developed in recent years.

1.2 Nuclear reactions

It is a mechanism in which two or more nuclei or else a nucleus and subatomic particles collides to form unlike products that are different from the earlier ones that initiate the process.

Nuclear reactions can be classified into two reactions i.e. Fusion reaction and fission reaction, which provides the significant information about the formation of new elements and their structure .The above practice generally subject to excitation energy, impact parameter, angular momentum, atomic masses, charges of the nuclei etc. The capability to explain all these phenomenon is complex as the nuclear interaction is not fully understood, though a significant amount of effort are already spend in studying it. The main motive of present work is to study the nuclear reaction via fusion process.

Fusion is defined as the reaction in which two or more atom collides with enough kinetic energy so that it can overcome the repulsion occurring between them and forms a new heavier nuclei with release of energy. The reason of release in energy is the difference in the mass of two products which is less than the mass of fissioning nuclei. The nuclei having atomic number greater than or equal to 2 and mass number greater than or equal to 4 are called heavy-ion. These nuclei are equal or heavier than α - particle. On the basis of energy of the incident particle (projectile) the nuclear reaction dynamics can be categorizes into low energy ($E \leq 15$ MeV/nucleon), intermediate energy ($15 < E < 1$ GeV/nucleon), and high energy ($E \geq 1$ GeV/nucleon). In this study, we worked on low energy reaction.

1.3 Low energy heavy ion reactions:-

During past few decades, low energy, heavy ion reaction is a topic of interest and have received greater attention in nuclear physics as it presents the information about the nuclear structure, nuclear forces and the nucleus-nucleus interaction. Heavy ion fusion reaction mechanism provides an opportunity to examine the barrier distribution and nucleus-nucleus potential.

The two forces i.e., Coulomb force and nuclear force will act on the interacting nuclei when they come close to each other from infinity. The Coulomb force is a long ranged force and it is due to the repulsion between the nuclei while the nuclear force is due to the attraction and is a short range force. To overcome the repulsive force the energy of the incident particle must be high enough to overcome a barrier which is called “Coulomb barrier” having an energy pocket inside it. Beside these two forces, centrifugal force is also present in heavy ion induced reactions. The nuclear structure effect are prominent in the region which is around and below the Coulomb barrier whereas, it fades at energies above the Coulomb barrier where centrifugal effect dominates.

When the collision of projectile and target takes place there is a formation of composite system, which leads to the formation of compound nucleus. In order to confine within the range of nuclear interaction the colliding nuclei should have sufficient energy. The formation of compound nucleus depends on interacting potential [2].

1.4 Nucleus-nucleus interaction potential: - For better understanding of any nuclear aspects, the fundamental key is nucleon-nucleon interaction. Heavy ion collision gives new possibilities for investigation of ion-ion interaction potential. To describe the interaction potential various models have been developed at microscopic/macroscopic level.

The total interaction potential comprises the sum of repulsive Coulomb force, centrifugal interaction and attractive nuclear potential.

The Fig.1 depicts the variation of different parts of total interaction potential plotted for the $^{19}\text{F} + ^{139}\text{La}$ reaction. The Coulomb and centrifugal interactions determines the long range part whereas the nuclear surface properties and readjustment of nuclear system is determined by the nuclear proximity potential. Both the Coulomb interaction and nuclear interaction plays an important role in the formation of compound nucleus (CN).

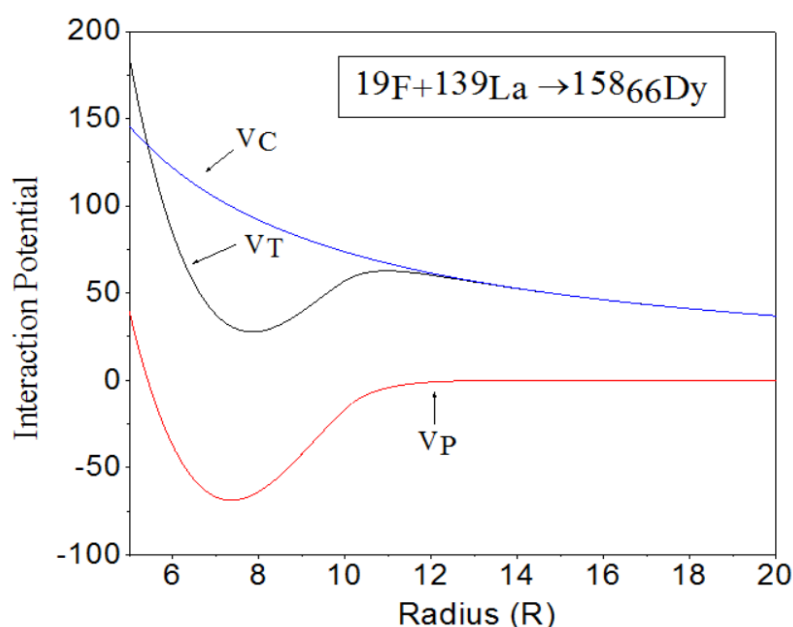


Fig.1.1:- Interaction potential for $^{19}\text{F} + ^{139}\text{La}$ reaction as a function of internuclear separation.

The study of nuclear interaction potential part is not well established in comparison to centrifugal and Coulomb part. The potential barrier cannot be described only by the Coulomb potential, a proper choice of nuclear potential is also required to study the heavy-ion reaction dynamics.

From the studies, it is obvious that experimentally, it is not possible to reveal the information about fusion barrier, it measures only fusion cross section [3]. The fusion barrier can be extracted by various theoretical models which gives the knowledge about the nuclear interaction at microscopic/ macroscopic level. Among various theoretical models, the ready to use pocket formula [4] from phenomenology are widely used by experimentalists and theoreticians.

The potential is parameterized by well-known quantities like charge, mass and isospin of colliding nuclei. Using several approaches the fusion barrier is parameterized by various authors [5, 8-10].

1.5 Proximity formalism:-

When the two surfaces are approaching each other within a distance of $< 2-3$ fm, or when at the time of separation nucleus distributes itself into two fragments, then both the surfaces face each other by short distance. When the two surfaces are brought into close proximity, then the strong attraction is not only due to surface energy term, an additional force due to proximity of the surface will also appear, which is known as proximity force [4]. The potential due to proximity force is known as “Proximity potential”.

The majority of phenomenological proximity potentials are based on proximity theorem, which shows that nuclear part of interaction potential can be taken as a product of factor that depends on the mean curvature of interaction surface and universal function that depends on separation distance. The universal function does not depend on the mass of the colliding nuclei but depend on the separation between their surfaces. The separation among the two colliding nuclei is associated to internuclear distance between centermost parts of the colliding nuclei from their nuclear radii.

The nucleus-nucleus interaction can be calculated and the fusion barrier can be parameterized by using various proximity potential [5]. These potentials are backbone of all microscopic/macrosopic models.

Firstly Bass [6-7] proposed an expression for nuclear interaction potential. Later on a formula of proximity potential was introduced by Blocki. *et.al.* [4], known as “pocket formula”, which presents the interaction energy of the nucleus as a function of separation between the surfaces of two colliding nuclei. In the nuclear reaction studies, the nuclear proximity potential is considered to be an interesting topic, so various versions of proximity potentials have been developed over the years [5], [8-10]. Few of these potentials have been able to explain the fusion barrier height and scattering data.

The Proximity Potential has gone under various modifications over the past few decades [11-12]. The experimental data was described by these modifications which further depend upon the surface energy coefficients or nuclear radius. Among various available versions for nuclear proximity potential we intend to use five potentials, which covers wide range of barrier characteristics, to study their effectiveness in different mass regions of the Periodic table.

1.6 Different mass regions: -

The various mass regions are categorized as follows:-

1.6.1 Lighter Mass Region: - The nuclei with mass number $A \leq 80$ lies in this mass region. The N/Z or neutron to proton ratio in chosen the reactions of this region is approximately equals to 1. Due to their small size, the effect of nuclear and the Coulomb potential is strong in this region.

1.6.2 Intermediate and Heavy Mass Region: - For the intermediate mass region, the mass of nuclei should lie in the region 80-190 for intermediate and 190-270 for heavy mass region.

The N/Z ratio for the elements of the reaction in this reaction is greater than 1, due to which the barrier height get decreased due to the addition of neutrons in the elements.

They deviates from the spherical shape to deformed shape, after the inclusion of deformation and orientation effect.

1.6.4 Super Heavy Mass Region: - The elements having mass greater than 270 lies in this region. After the deformation effect, they formed highly deformed nuclei which reduces the barrier height. In this region, the Coulomb and proximity potential is modified by the multipole deformations.

1.7 Deformation and Orientation Effects:-

Deformation and orientation are important aspects in the study of nuclear fusion reactions dynamics. The shapes of target and projectile changes the interaction barrier during the fusion reaction. Hence it is important to account the contribution of deformation along with their orientation degree of freedom.

Majority of the nuclei deviates from the spherical shape and these deformation are defined on the basis of electric quadrapole deformation. The nuclei are supposed to possess mainly deformations such as quadrapole, octupole and hexadecapole shown in the Fig.1.2.

The amount at which the nucleus is deformed can be provided by a deformation parameter β_λ , where β is an amplitude of how much scissioning nucleus is different from spherical shape and λ corresponds to the order of deformation. The value of λ can be 2, 3 and 4.

The quadrapole deformation are further classified into prolate deformed ($Q > 0$) and oblate deformed $Q < 0$, nuclei, where Q is the electric quadrapole moment is shown in Fig.1.2.

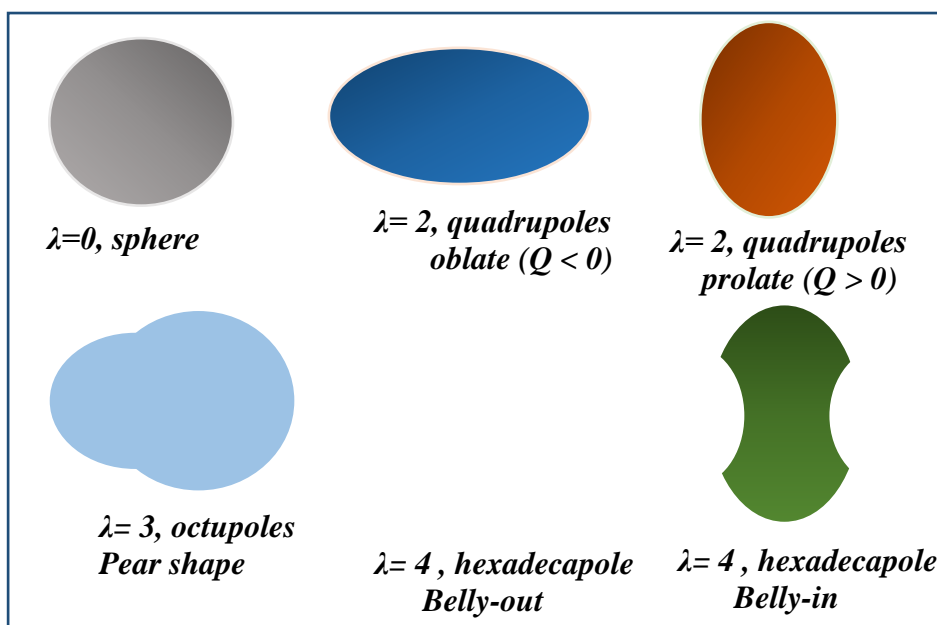


Fig.1.2:- Multipole deformations along with their shapes

The orientation of these deformed nuclei also plays major contribution in reaction dynamics. Gupta and his co-workers in their research work [15] explained the influence of deformed and oriented nuclei on interaction barrier i.e. height and its position. In order to analyse the optimum effect of all the orientation, the optimum orientations have been calculated for the fusion reactions, which are defined as “Cold – non compact or elongated” orientation and “Hot- compact or flattened” orientation as shown in Fig.1.3.

The “Hot-compact” configuration refers to large barrier height and lower interaction radius while the “cold- non compact” configuration leads to lower barrier height and large interaction radius [13-15].

To establish the effect of deformation and orientation on fusion reaction there is a need of experimental and theoretical study of collision between deformed and oriented nuclei [18-21].

The Fig. 1.3 depicts the deformation of the prolate-prolate and oblate-oblate colliding nuclei on collision axis for both “cold-non compact” and “hot-compact” configuration.

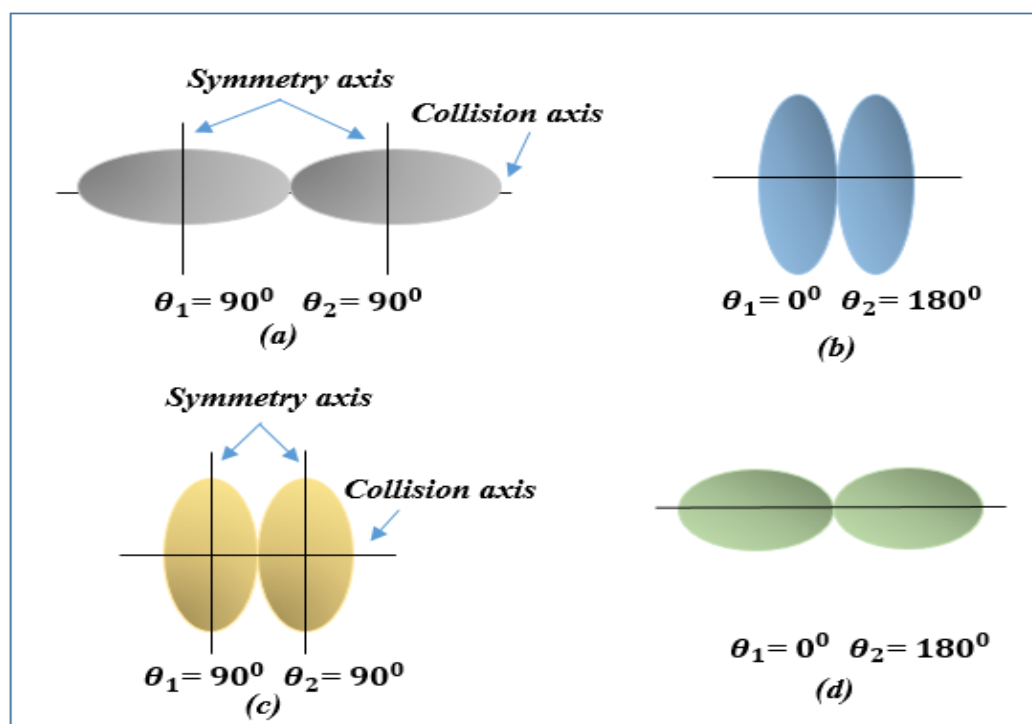


Fig.1.3:- The deformation of the ((a), (b) oblate and (c), (d) prolate) colliding nuclei on collision axis for both “cold-non compact” ((a), (d)) and “hot-compact” configuration ((b), (c)).

This specification had been shown in the Ref. [15], but our present work is based on “hot compact” configuration.

Mostly quadrupole deformations affect the fusion anomalies and therefore our current work is restricted to quadrupole deformations only.

But mostly quadrupole deformations affect the fusion anomalies and therefore our current work is restricted to quadrupole deformations only.

In the fusion reaction due to the deformation in the nuclei, the barrier height is lowered which delivered an easier way for the formation of compound nucleus. Likewise, orientations change the Coulomb barrier along with the centers between the two colliding nuclei. So, the deformation along with the orientation are necessary for the study of the nuclear reaction dynamics. In the present work, the role of deformation and optimum orientation is also analyzed in different mass regions.

References:-

1. J. J. Thomson, Phil. Mag **44**, 293 (1897).
2. N. Bohr, Nature (London) **137**, 344 (1936).
3. L. F. Canto, P. R. S. Gomes, R. Donangelo and M. S. Hussein, Phys. Rep. **424** (2006).
4. J. Blocki, J. Randrup, W. J. Swiatecki and C.F.Tsang, Ann. Phys. (NY) **105**, 427 (1977).
5. I. Dutt & R K. Puri, Phys. Rev. C **81**, 064609 (2010).
6. R. Bass, Nucl. Phys. A **231**, 45 (1974).
7. R. Bass, Nuclear Reactions with Heavy-ions (Springer- Verleg, Berlin, 1980).
8. J. Randrup and J. S. Vaagen, Phys. Lett. B **77**,170(1978).
9. M. Seiwert, W. Greiner, V. Oberacker and M. J. Rhoaes-Brown, Phys. Rev. C **29**, 477 (1984).
10. J. R. Birkelund and J. R. Huizenga, Phys. Rev. C **17**, 126 (1978).
11. W. Reisdorf, J. Phys. G: Nucl. Part. Phys. **20**, 1297 (1994).
12. W. D. Myers and W. J. Swiatecki, Phys. Rev. C **62**, 044610 (2000).
13. N. Malhotra and R. K. Gupta, Phys. Rev. C **31**, 1179 (1985).
14. A. Iwamoto, P. Moller, J. R. Nix, and H. Sogawa, Nucl.Phys. A **596**, 329-354 (1996).
15. R. K. Gupta, M. Balasubramaniam, R. Kumar, N. Singh, M. Mahhas, and W. Greiner, J. Phys. G: Nucl. Part. Phys. C **31**, 631 (2005).

16. M. Manhas and R. K. Gupta, Phys. Rev. C **72**,024606 (2005).
17. R. K. Gupta, M. Manhas ,G. Munzenberg and W. Greiner, Phys. Rev. C **72**, 014607 (2005).
18. K. Nishio, H. Ikezos, S. Mitsuoka and K. Satou and S.C. Jeong , Phys. Rev. C **63**, 044610 (2001).
19. D. J. Hinde, M. Dasgupta , J. R. Leigh, J.P. Lestone, J.C. Mein, C.R. Morton, J.O. Newton, and H. Timmers, Phys. Rev. Lett. **74**, 1295(1995).
20. M. Dasgupta, D. J. Hinde, J. R. Leigh and K. Hagino, Nucl. Phys. A **630**, 78C (1998).
21. Yu. Ts. Oganessian, Heavy Elements and Related New Phenomena, edited by W. Greiner and R. K. Gupta, World Scientific, Singapore, P.**43**,(1999).

Methodology:-

The details of total interaction potential and contributing terms are presented in Sec. 2.1. For the calculation of fusion cross section the Wong formula is used. The corresponding details are given in subsequent Sec. 2.2.

2.1 Total Interaction Potential: - The total interaction potential is the sum of long range Coulomb potential, angular momentum dependent potential and proximity potential and it can be written as

$$V_l^T(R, E_{c.m}, \theta_i) = V_C(R, Z_i, \beta_i, T, \theta_i) + V_l(R, A_i, \beta_i, T, \theta_i) + V_N(R, A_i, \beta_i, T, \theta_i) \quad (2.1)$$

Here V_C , V_l, V_N are the temperature, deformations and orientations dependent Coulomb potential, angular momentum dependent potential (centrifugal potential) and proximity potential respectively.

The detail of each part of total interaction potential is discussed below:

2.1.1 Coulomb potential: - The repulsive force acting between two interacting nuclei defines

the Coulomb potential. The Coulomb potential between the two spherical nuclei is given by

$$V_C = \frac{Z_1 Z_2 e^2}{R} \quad (2.2)$$

If the interacting nuclei are deformed then the Coulomb potential is given by [11]:-

$$V_C = \frac{Z_1 Z_2 e^2}{R} + 3Z_1 Z_2 e^2 \sum_{\lambda, i=1,2} \frac{R_i^\lambda(\alpha_i)}{(2\lambda+1)R^{\lambda+1}} Y_\lambda^0(\theta_i) [\beta_{\lambda i} + \frac{4}{7} \beta_{\lambda i}^2 Y_\lambda^0(\theta_i)] \quad (2.3)$$

Here θ_i represents the orientation angle measured from the collision axis and symmetry axis to the axis of collision in the anti-clock wise direction. α_i is the angle measured in clockwise direction between the symmetry axis and radius vector of colliding nuclei from symmetry axis. $Y_\lambda^0(\theta_i)$ denotes the spherical harmonics functions. $\beta_{\lambda i}$ signifies deformation parameter taken from the table of Moller *et al.* [2] with “hot-compact” optimum orientations taken from the table of Gupta *et al.* [1].

2.1.2 Angular momentum dependent potential: -

Due to angular momentum effect the rotational energy is defined as:-

$$V_L = \frac{\hbar^2 l(l+1)}{2I(T)} \quad (2.4)$$

Here $\mu = \frac{A_1 A_2}{A_1 + A_2} m$ is the reduced mass with m is the nucleon mass and $I = \mu R^2$. is the moment of inertia calculated in non-sticking limit.

2.1.3 Proximity potential for deformed and oriented nuclei. :-

As discussed in chapter 1 that when two surfaces come in contact within a distance of < 2 fm, then a force come into play which bring them into closed proximity, which is called proximity force. The potential due to these forces are called proximity potential. A wide range of these types of potentials are available. But in the present work, a set of five potentials are considered as these covers a wide range of barrier characteristics. A detail of various proximity potential used in are present work is given below.

Proximity 1977 (Blocki): Blocki *et al.* [3] proposed that the force between the two surfaces in close proximity is proportional to interaction potential per unit area. The proximity potential (V_N) for hot, deformed and oriented nuclei is given as [4]:-

$$V_N(A_i, \beta_{\lambda i}, \theta_i, T) = 4\pi \bar{R} \gamma b(T) \Phi(s_0(T)) \quad (2.5)$$

Here $\Phi(s_0)$ is the universal function, which is independent of the shape of the nuclei but it depends upon s_0 i.e. separation distance, b and \bar{R} are the surface diffuseness parameter and mean curvature radius respectively.

$$\phi(s_0) = \begin{cases} -\frac{1}{2}(s_0 - 2.54)^2 - 0.0852(s_0 - 2.54)^3, & s_0 \leq 1.2511 \\ -3.437 \exp\left(-\frac{s_0}{0.75}\right), & s_0 \geq 1.2511 \end{cases} \quad (2.6)$$

Here s_0 is represented in terms of b i.e. $s_0 = \frac{s_0}{b}$. It is defined for negative, zero and positive values of s_0 (distance of closest approach) [5].

The surface energy coefficient γ is given by:-

$$\gamma = \gamma_0 \left[1 - k_s \left(\frac{N-Z}{A} \right)^2 \right] \quad (2.7)$$

where γ_0 and k_s are the surface energy coefficient and surface energy constant. In the present version the value of γ_0 and k_s are 0.9517 MeV/fm^2 and 1.7826 . Here N and Z are the total number of neutrons and protons.

The radius vector R_i can be written as

$$R_i = \left[1.8 A_i^{-1/3} - 0.76 + 0.8 A_i^{-1/3} \right] (1 + 0.0007 T^2), (i = 1, 2). \quad (2.8)$$

Here temperature T is related to energy by following expression:

$$E_{CN}^* = \frac{A}{a} T^2 - T, \quad (2.9)$$

where $a = 9-10$, depending on the mass A of CN.

Proximity 1988 (Prox88):- This formula was introduced by Moller and Nix [6] by modifying the value of coefficients as $\gamma_0 = 1.2496 \text{ MeV/fm}^2$ and $k_s = 2.3$. This modified version is referred as ‘‘Proximity 1988’’. This parameter set give deeper pocket and stronger isospins effect in comparison to Prox 77.

Bass 1980 (Bass80):- The nuclear interaction potential $V_N(R)$ can be written as:-

$$V_N(R) = \frac{R_1 R_2}{R_1 + R_2} \phi(s) \quad (2.10)$$

where, $s = r - R_1 - R_2$, the universal function $\phi(s)$ for this potential [7] is in the form as:-

$$\phi(s) = \left[0.033 \exp\left(\frac{s}{3.5}\right) + 0.007 \exp\left(\frac{s}{0.65}\right) \right]^{-1} \quad (2.11)$$

with central radius, R_i as

$$R_i = R_s \left(1 - \left(\frac{0.98}{R_s^2} \right) \right), (i = 1,2) \quad (2.12)$$

Christensen and Winther 1976 (CW 76):- Based on semi-classical approach, the nuclear interaction was derived by Christensen and Winther [8]. The nuclear proximity interaction for this potential can be written as:-

$$V_p = -50\bar{R}\phi(R - R_1 - R_2) \quad (2.13)$$

where \bar{R} with

$$R_i = \left[1.233A_i^{\frac{1}{3}} - 0.978A_i^{\frac{-1}{3}} \right], (i = 1,2) \quad (2.14)$$

The universal functions $\phi(s = R - R_1 - R_2)$, is

$$\phi(s) = \exp\left(\frac{-s}{0.63}\right) \quad (2.15)$$

Broglia and Winther 1991(BW 91):- This potential is the modified version of CW 1976 and was derieved by Broglia and Winther [9]. The nuclear proximity interaction for this potential can be written as:-

$$V_p(R) = \frac{-V_0}{1 + \exp\left(R - \frac{R_0}{0.63}\right)} MeV \quad (2.16)$$

with $V_0 = 16\pi\bar{R}\gamma a$ where $a = 0.63$ fm, $R_0 = R_1 + R_2 + 0.29$

and

$$R_i = \left[1.233A_i^{\frac{1}{3}} - 0.978A_i^{\frac{-1}{3}} \right], (i = 1,2) \quad (2.17)$$

The surface energy constant used for this potential is:-

$$\gamma = \gamma_0 \left[1 - k_s \left(\frac{N_1 - Z_1}{A_1} \right) \left(\frac{N_2 - Z_2}{A_2} \right) \right] MeV fm^{-2} \quad (2.18)$$

Here N and Z are the total number of neutrons and protons .The value of γ_0 and k_s taken to be 0.95 MeV/ fm² and 1.8.

2.2 Wong Formula

At sub barrier energies the cross section for fusion of two nuclei have been determined at a large scale. It was observed that the magnification of cross section get affected at near and below the Coulomb barrier and from this determination the nucleus-nucleus interaction can be observed. This explanation of cross section leads to the penetration of one - dimensional barrier. This barrier governs the fusion and gives some parameters of potential barrier. The cross section can be find by changing these parameters [10].

According to Wong [11], for the two deformed and oriented nuclei, which lie in the same plane and collides with center of mass with energy $E_{c.m}$, the fusion cross section in the form of angular momentum partial waves, can be written as:-

$$\sigma(E_{c.m}, \theta_i) = \frac{\pi}{k^2} \sum_{l=0}^{\infty} (2l + 1) P_l (E_{c.m.}, \theta_i) \quad (2.19)$$

where, $k = \sqrt{\frac{2\mu E_{c.m.}}{\hbar^2}}$, μ is the reduced mass and P_l is the transmission coefficient which describes the penetration of barrier.

The penetrability P_l in terms of its height $V_B^l(E_{c.m}, \theta_i,)$ and curvature $\hbar\omega_l(E_{c.m}, \theta_i,)$ is

$$P_l = [1 + \exp\left(\frac{2\Pi(V_B^l(E_{c.m.}, \theta_i) - E_{c.m.})}{\hbar\omega_l(E_{c.m.}, \theta_i)}\right)]^{-1} \quad (2.20)$$

with $\hbar\omega_l(E_{c.m}, \theta_i, \phi)$ estimated at the barrier position $R=R_B^l$ corresponding to the maximum barrier height $V_B^l(E_{c.m}, \theta_i, \phi)$, given as

$$\hbar\omega_l(E_{c.m}, \theta_i,) = \hbar \left[\left| \frac{d^2 V_l(R)}{dR^2} \right|_{R=R_B^l} / \mu \right]^{1/2} \quad (2.21)$$

and, the R_B^l obtained from the condition

$$|dV_l(R)/dR|_{R=R_B^l} = 0 \quad (2.22)$$

Wong carried out the ℓ summation under the condition as follows:-

- (i) $\hbar\omega_\ell \approx \hbar\omega_0$
- (ii) $V_B^l \approx V_B^0 + \frac{\hbar^2\ell(\ell+1)}{2\mu R_B^{02}}$, Which means to assume $R_B^l \approx R_B^0$.

Both V_B^l and $\hbar\omega_\ell$ are obtained in terms of its $\ell = 0$ Values, with V_B^0 gives as the sum of nuclear proximity potential V_P and Coulomb potential V_C at

$$V_B = V_P(R = R_B^0, A_i, \beta_{\lambda i}, E_{c.m}, \theta_i) + V_C(R = R_B^0, Z_i, E_{c.m}, \theta_i) \quad (2.23)$$

where $\beta_{\lambda i}, \lambda = 2,3,4$ are the multipole deformations.

Using the above two approximations and integrating over ℓ , gives the Wong formula [11].

$$\sigma(E_{c.m}, \theta_i, \phi) = \frac{R_B^0 \hbar\omega_0}{2E_{c.m}} \ln \left[1 + \exp \left(\frac{2\pi}{\hbar\omega_0} (E_{c.m} - V_B^0) \right) \right] \quad (2.24)$$

which on integration over the orientation angle θ_i ($\alpha = 1,2$) gives the fusion cross section

$$\sigma(E_{c.m}) = \int_{\theta_1, \theta_2=0}^{\pi/2} \sigma(E_{c.m}, \theta_i) \sin \theta_1 d\theta_1 \sin \theta_2 d\theta_2 \quad (2.25)$$

References:-

1. R. K. Gupta, M. Balasubramaniam, R. Kumar, N. Singh, M. Manhas and W. Grenier, *J. Phys. G: Nucl. Part. Phys.* **31**, 631 (2005).
2. P. Moller, J. R. Nix, W. D. Myers, W. J. Swiatecki, *At. Data Nucl. Data Tables* **59**, 85 (1995).
3. J. Blocki, J. Randrup, W. J. Swiatecki and C. F. Tsang, *Ann. Phys. (N.Y.)* **105**, 427 (1977).
4. R. K. Gupta, N. Singh and M. Manhas *Phys. Rev. C* **70**, 034608 (2004).
5. G. Royer and J. Mignen, *J. Phys. G: Nucl. Part. Phys.* **18**, 1781 (1992).
6. P. Moller and J. R. Nix, *Nucl. Phys. A* **361**, 117 (1981).
7. W. Reisdorf, *J. Phys. G: Nucl. Part. Phys.* **20**, 1297 (1994).
8. P. R. Christensen and A. Winther *Phys. Lett. B* **65**, 19 (1976).
9. W. Reisdorf, *J. Phys. G: Nucl. Part. Phys.* **20**, 1297 (1994).
10. A. B. Balantekin, S. E. Koonin and J. W. Negele, *Phys. Rev. C*, Vol. **28**, 4 (1983).
11. C. Y. Wong, *Phys. Rev. Lett.* **31**, 766 (1973).

Result and Discussion

3.1 Introduction

In this chapter, the effect of different types of proximity potential on the fusion excitation function is analyzed for the various reactions taken from different mass regions of the periodic table. It is generally observed that with increase in mass region, the sub barrier fusion anomalies increases across the Coulomb barrier. This might be due to the nuclear structure effect which plays prominent role in sub-barrier regions. However, at above barrier regions, the nuclear structure effect fades down with the dominance of centrifugal effect. Hence, in order to deal with fusion probability at low energies, proximity potential plays an important role in heavy-ion reactions.

A variety of nuclear proximity potential have been derived on the basis of proximity theorem and are studied extensively in recent years [1-3], which confirms their effectiveness in complete understanding of fusion mechanism. Making use of above information, here five proximity potential namely Prox 77, Prox 88, Bass 80, BW 91 and CW 76 , which covers the wide range of barrier characteristics have been used in the present work.

In this chapter we first investigate the effect of deformation and orientation on the barrier characteristics by using above mentioned proximity potential to be discussed in Sec. 3.2. In Sec 3.3, the fusion cross section are calculated with the Wong formula [4], using above mentioned proximity potential in different mass regions. Two different sets of reaction corresponding to the light, intermediate, heavy and super heavy mass regions are chosen for the analysis.

3.2 Interaction potentials using different proximity potential: -

The Coulomb potential along with the nuclear potential is required for obtaining the fusion barrier height (V_B) and the barrier position (R_B). Experimentally, the Coulomb barrier height and its position cannot be measured directly.

The typical fusion excitation functions are attained by fitting the experimental data with the Wong formula and the appropriate parameters including the barrier height, position and curvature are extracted. The fusion barrier height gets modified significantly for the deformed nuclei in comparison to the spherical choice of nuclei [3].

Fig. 3.1 depicts the interaction potential for the reaction $^{16}O+^{176}Yb$ at $T=0$ (a) considering spherical and (b) deformed choice of nuclei using different nuclear proximity potentials namely Prox 77, Prox 88, Bass 80, BW 91, CW 76. These potentials are considered as they cover entire range of barrier characteristics.

In Fig. 3.1(a), for the spherical case, it is clearly seen that the barrier profiles of different potentials BW 91, Bass 80, Prox 77, Prox 88 and CW 76 are different. Here the highest barrier correspond to BW 91 and CW 76 whereas lowest barrier corresponds to Prox 88. On the inclusion of deformation along with the optimum orientations the barrier profiles get significantly affected [5]. From Fig. 3.1(b), it is noticed that BW 91 yields the highest barrier while, the barrier characteristics of Bass 80 and CW 76 shows quiet similar behavior with barrier higher than Prox 77. However, Prox 88 in resemblance to the spherical case shows the lowest barrier.

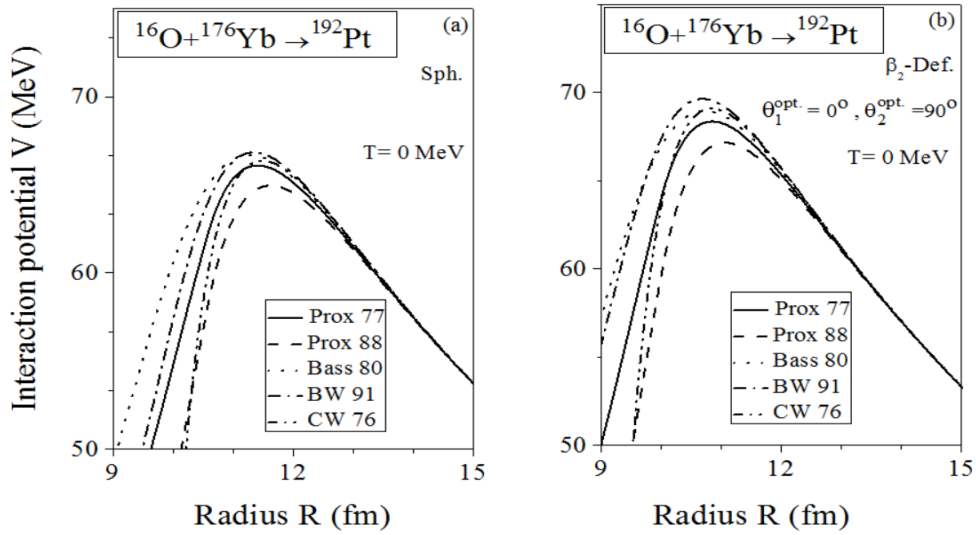


Fig 3.1 :- Total interaction potential calculated $V(\text{MeV})$ as a function of radius $R(\text{fm})$ for $^{16}\text{O}+^{176}\text{Yb}$ reaction using Prox 77, Prox 88, Bass 80, BW 91, CW 76 potentials at $T=0$ for (a) the spherical and (b) deformed choice of nuclei along with the optimum orientations.

Hence, the consequences of deformation on barrier characteristics combined with the use of distinct proximity potential deliver an interesting input to recognize the formation procedure in various nuclear reactions which covers the wide mass range.

3.3 Fusion cross-section in different mass regions of periodic table using various proximity potential:-

In this section, we investigate the effect of different proximity potentials by calculating the fusion cross section of various reactions using the Wong formula. Each reaction is taken from different mass regions of the periodic table i.e. $^{28}\text{Si} + ^{28}\text{Si}$, $^{74}\text{Ge} + ^{74}\text{Ge}$, $^{16}\text{O} + ^{176}\text{Yb}$ and $^{27}\text{Al} + ^{238}\text{U}$ corresponding to lighter, intermediate, heavy and super-heavy mass region respectively.

The calculated fusion cross sections using different proximity potentials have been compared with experimental data [6-9].

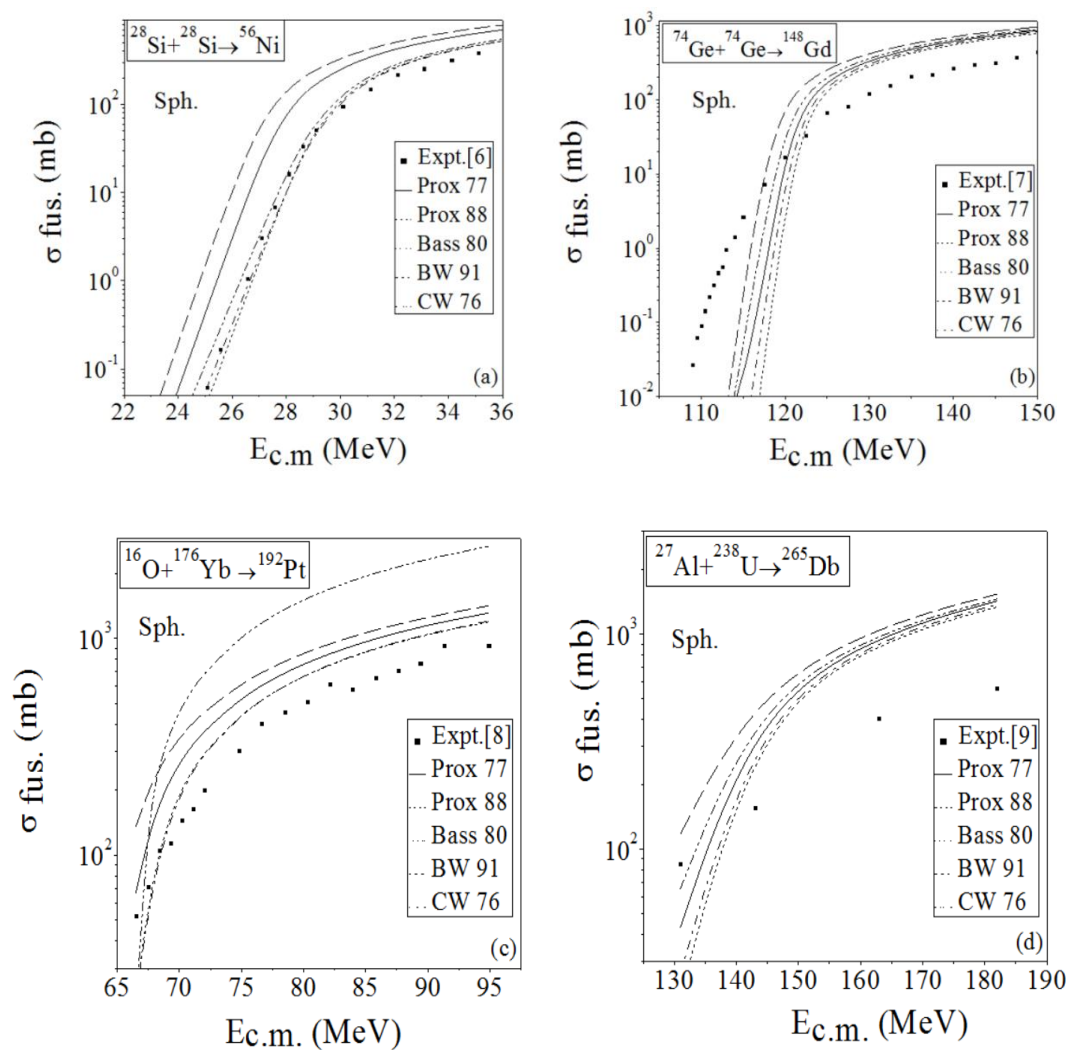


Fig. 3.2 Fusion excitation function using various proximity potential for the reactions (a) $^{28}\text{Si} + ^{28}\text{Si}$, (b) $^{74}\text{Ge} + ^{74}\text{Ge}$, (c) $^{16}\text{O} + ^{176}\text{Yb}$ and (d) $^{27}\text{Al} + ^{238}\text{U}$ calculated with the Wong formula considering spherical choice of nuclei and compared with the available experimental data [6-9].

Firstly, considering spherical choice of nuclei, the variation of fusion cross section is analyzed at energies below and above the Coulomb barrier as shown in Fig. 3.2 for different mass regions using various proximity potentials

It is observed that for lighter mass region i.e. for $^{28}\text{Si} + ^{28}\text{Si}$ reaction as shown in Fig.3.2 (a), the proximity potentials BW 91 and Bass 80 with highest barrier gives relatively better agreement with experimental data at energies below as well as above the Coulomb barrier. While the potentials namely Prox 77, Prox 88 and CW 76 with their lowest barrier overestimates the experimental data.

We further checked the behavior of these potentials in intermediate mass regions for the reaction $^{74}\text{Ge} + ^{74}\text{Ge}$ in Fig. 3.2(b), and it is observed that in this mass region, the performance of proximity potentials gets changed. Here the potential with highest barrier i.e. BW 91 and CW 76 and Prox 77 perform badly in sub- barrier region. While the potential with lowest barrier i.e. Prox 88 shows close agreement with experimental values below the barrier whereas Bass 80 matches the experimental data for above barrier energies.

The role of different proximity potentials is further analyzed in the heavy mass region for the reaction $^{16}\text{O} + ^{176}\text{Yb}$ in Fig.3.2 (c). From this figure, it is observed that the proximity potentials exhibiting highest barrier namely BW 91 and Bass 80 shows better agreement in reference to experimental fusion cross- section at below and above the Coulomb barrier, while the other potentials like CW 76, Prox 77 and Prox 88 overestimates the experimental data due to their lower barrier.

This behavior seems to be consistent in the super- heavy mass region for the reaction $^{27}\text{Al} + ^{238}\text{U}$ as shown in Fig.3.2 (d). For this reaction, BW 91, Prox 77 and Prox 88 underestimates the experimental data below the coulomb barrier. However, below the barrier CW 76 and above the barrier Bass 80 perform better in reference to experimental values.

As discussed earlier, the deformation and orientation significantly affect the barrier characteristics which consequently affect the fusion cross-section. For the deformed choice of nuclei the effect upto β_2 has been included with optimum choice of orientation and fusion cross section has been calculated by integrating over the orientation angles. The reactions mentioned above have been analyzed with inclusion of deformation and orientation and accordingly fusion cross section has been calculated and compared with available experimental data as shown in Fig. 3.3.

In Fig. 3.3, fusion excitation functions have been calculated by including the effect of deformation and orientation for the different mass regions: $^{28}\text{Si} + ^{28}\text{Si}$, $^{74}\text{Ge} + ^{74}\text{Ge}$, $^{16}\text{O} + ^{176}\text{Yb}$ and $^{27}\text{Al} + ^{238}\text{U}$. From this figure, it is clear that the fusion excitation function shows the similar result as for spherical case. In the lighter mass region (see Fig. 3.3(a)), the potentials Bass 80, BW 91 and CW 76 due to their higher barrier, gives comparatively better with experimental data at energies across the Coulomb barrier. Here, Bass 80 behaves better below the barrier and CW 76 above the barrier. While the Prox 77 and Prox 88 with their lower barrier overestimates the data to a larger extent.

The behavior of these potentials further changed in intermediate mass region for the reaction $^{74}\text{Ge} + ^{74}\text{Ge}$ as shown in Fig. 3.3(b). From this figure, we see that the fusion excitation functions calculated with Bass 80 and Prox 77 lie comparatively closer to the experimental values while BW 91 and CW 76 shows the similar result and Prox 88 due to their lower barrier overestimates the experimental fusion cross section on larger scale.

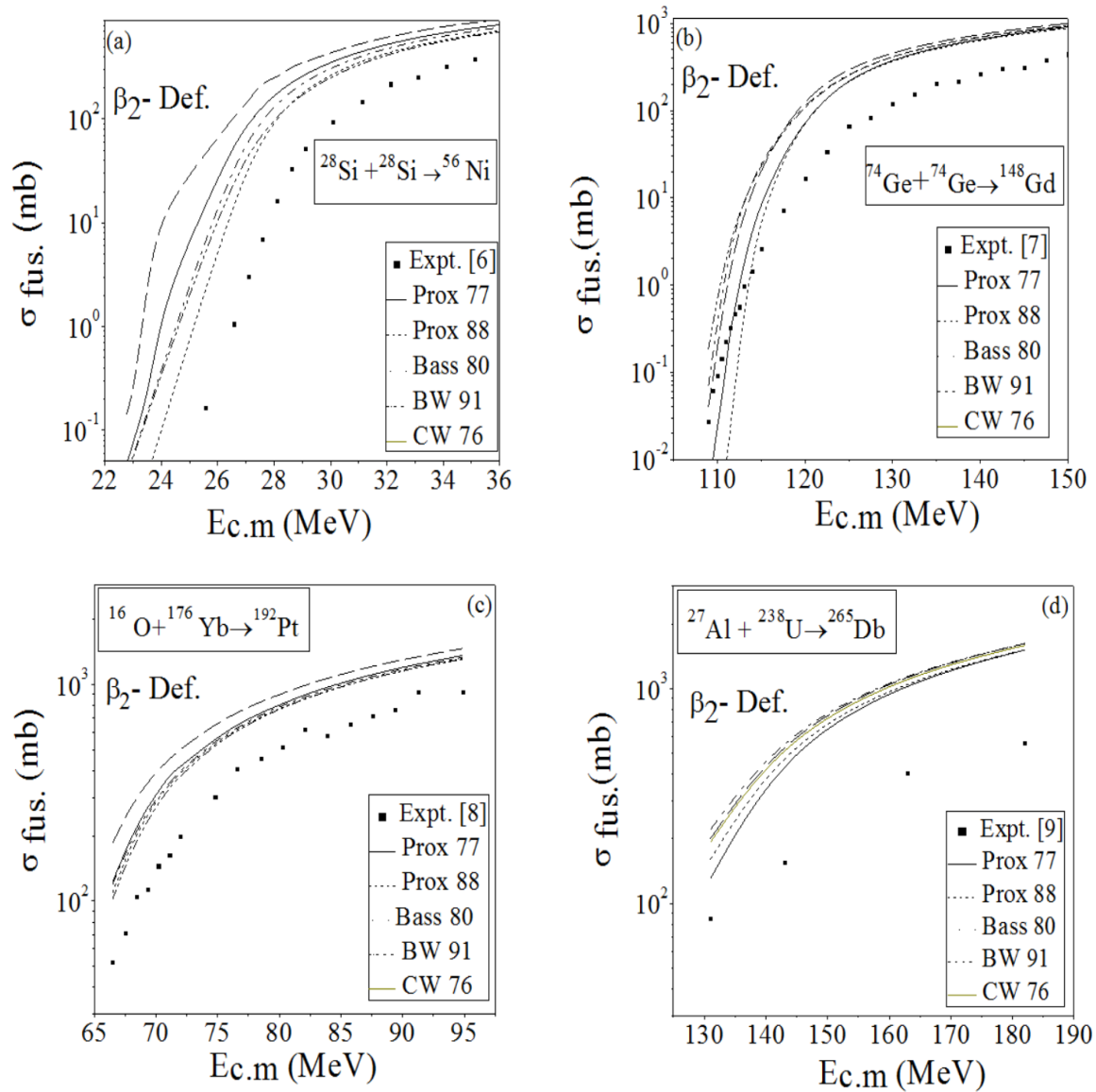


Fig. 3.3:- Same as Fig. 3.2 but for deformed choice of nuclei.

The effect of these potentials are further analyzed in heavier mass region for the reaction $^{16}\text{O} + ^{176}\text{Yb}$ shown in the Fig. 3.3(c). From this figure, it is observed that the fusion excitation functions show the similar behavior as for the spherical case.

Here, CW 76 and Bass 80 shows value close to the experimental data as compared to other potentials but BW 91, Prox 77 and Prox 88 overestimates the same.

As we move further and check the performance of these potentials in super-heavy mass region for the reaction $^{27}\text{Al} + ^{238}\text{U}$ in Fig.3.3 (d), we have examined that the fusion excitation functions calculated with the deformed choice of nuclei shows consistent behavior with the spherical choice. In this region, all the potentials i.e. Prox 77, Prox 88, Bass 80, BW 91 and CW 76 shows the similar behavior and overestimates the experimental values but we choose Prox 77 as the best option as it yields relatively closer values to the experimental data.

In order to check the above mentioned observations, there is a need to take another set of reactions each corresponding to different mass regions. In this set, we have chosen the reaction $^{28}\text{Si} + ^{30}\text{Si}$ from lighter mass region, $^{64}\text{Ni} + ^{130}\text{Te}$ from intermediate mass region, $^{19}\text{F} + ^{139}\text{La}$ from heavy mass region and $^{35}\text{Cl} + ^{238}\text{U}$ from super heavy mass region. The fusion excitation functions for these reactions using various proximity potential are calculated with spherical choice as well as deformed choice of nuclei and are compared with experimental data [6, 9 -11] corresponding results are shown in Fig 3.4 and Fig. 3.5 respectively.

For the reaction, i.e. $^{28}\text{Si} + ^{30}\text{Si}$ in the lighter mass region in Fig. 3.4 (a), Bass 80 and BW 91 and CW 76 are found to perform better at above and below the Coulomb barrier energies. Whereas Prox 77 and Prox 88 overestimates the experimental data due to their lower barrier height.

In the intermediate mass region, the result for the reaction $^{19}\text{F} + ^{139}\text{La}$ is shown in Fig.3.4 (b). From this figure, it is evident that the fusion excitation function for the reaction $^{19}\text{F} + ^{139}\text{La}$ behaves differently as compared to the intermediate mass region reaction of Set-I shown in Fig. 3.2(b). In the present case, the fusion excitation functions calculated for different proximity potentials are closer to experimental data as compared to that of Fig. 3.2(b). Out of different choice of proximity potentials, Prox 77 seems a good choice to analyze the fusion cross section at below barrier energy regime. While above the barrier BW 91 and Bass 80 shows the comparative result whereas Prox 88 overestimates the data

These potentials are further checked for heavy mass region corresponding to the reaction $^{64}\text{Ni} + ^{130}\text{Te}$ displayed in Fig. 3.4(c). In this mass region, Bass 80, BW 91 and Prox 77, provides better choice in estimating the experimental values at lowest incident energy after that it over estimates. A closer look at Fig.3.4 (c) suggests that Bass 80 perform better as compared to other potentials. While CW 76 and Prox 88 overestimates the experimental data. The result are consistent with the intermediate mass region reaction of first set shown in Fig.3.3 (c).

Further analysis is carried out in super heavy mass region for the reaction $^{35}\text{Cl} + ^{238}\text{U}$ in Fig 3.3(d). Here we conclude that all the proximity potentials exhibits the similar behavior but one should prefer to choose BW 91 below the barrier as it is more closer to the experimental data and Bass 80 performs well prefer to above the barrier.

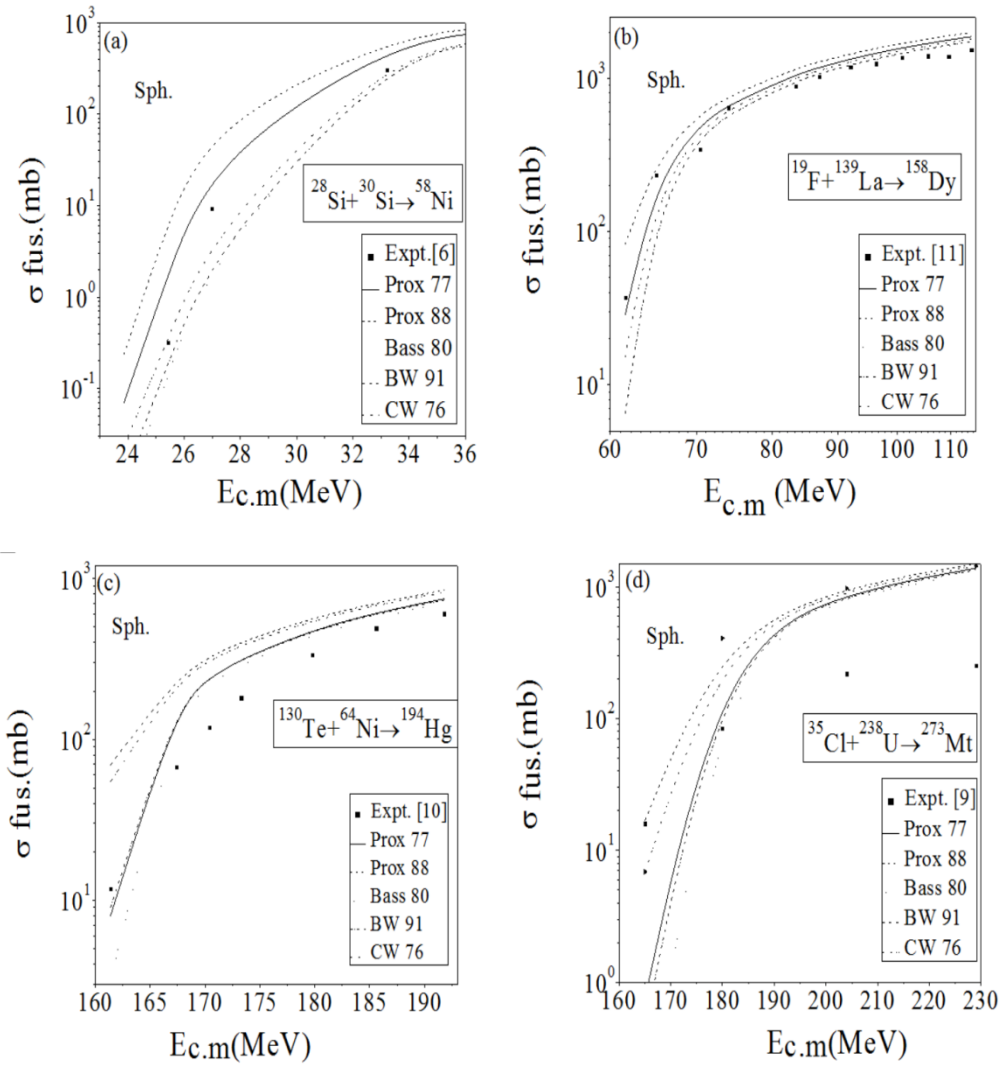


Fig. 3.4 :- Fusion excitation function using various proximity potential for the reactions (a) $^{28}\text{Si} + ^{30}\text{Si}$, (b) $^{19}\text{F} + ^{139}\text{La}$, (c) $^{130}\text{Te} + ^{64}\text{Ni}$, and (d) $^{35}\text{Cl} + ^{238}\text{U}$ calculated with the Wong formula considering spherical choice of nuclei and compared with the experimental data [6, 9-11].

In Fig. 3.5, the effect of deformations and orientation are switched on for the second set of reactions and fusion excitation function are calculated using different choices of proximity potentials.

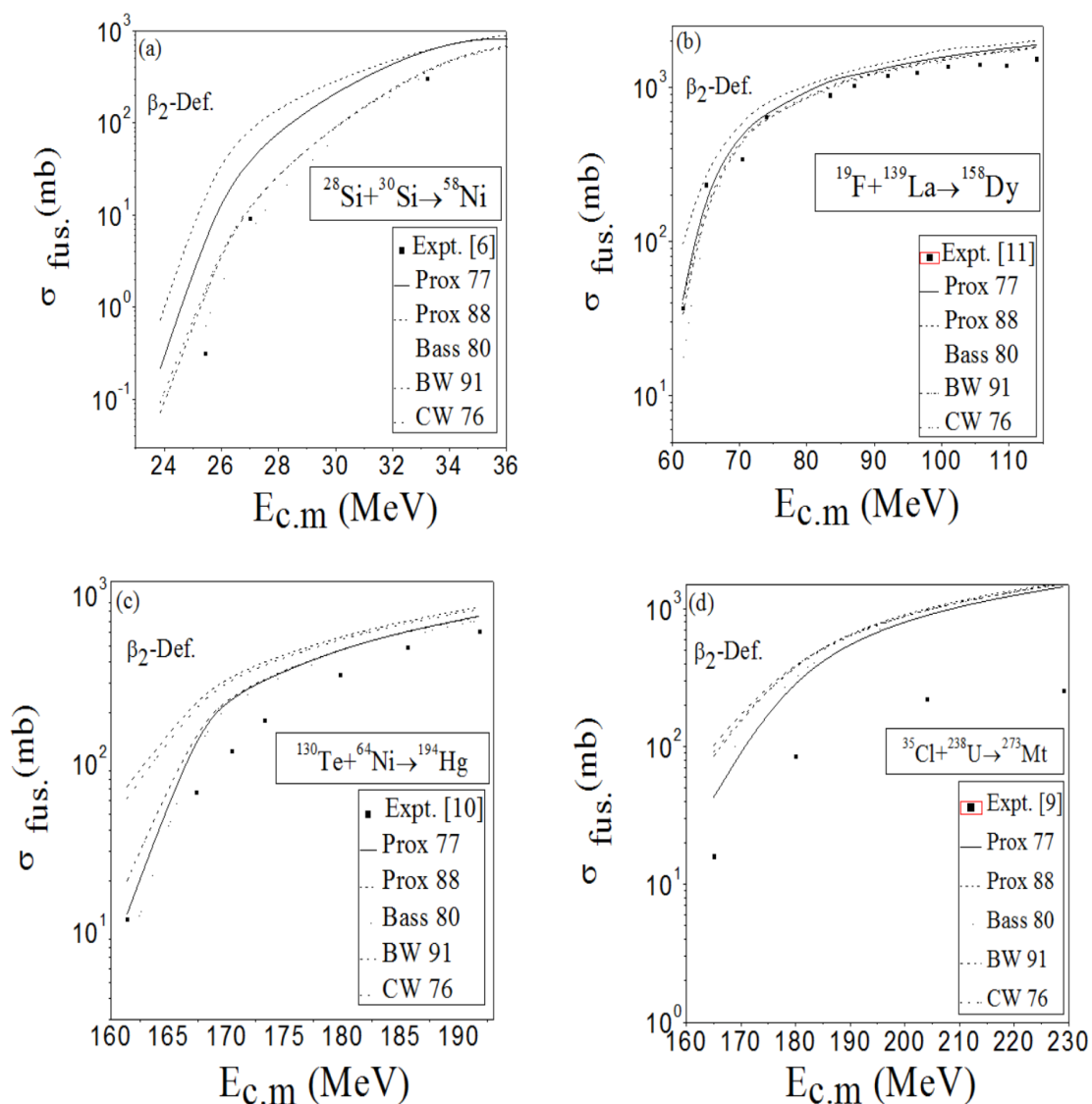


Fig. 3.5:- Same as Fig. 3.4 but for deformed choice of nuclei.

Firstly, in the lighter mass region, for the reaction $^{28}\text{Si} + ^{30}\text{Si}$ the fusion excitation functions with the consideration of deformations are shown in Fig. 3.5(a). Inclusion of deformation in the lighter mass region does not affect the results significantly. Here also Bass 80, BW 91 and CW 76 expresses the fair behavior in reference to experimental data whereas Prox 88 and Prox 77 overestimates the experimental data and behaves badly in addressing the same.

In the intermediate mass region for the reaction $^{19}\text{F} + ^{139}\text{La}$ the results are shown in Fig.3.5 (b), In this case, different proximity potentials act differently at near sub – barrier energies. All the potentials show different comparative result but out of these potentials one choose CW 76 and Prox 77 as it best fits the corresponding experimental data. Here also the results with deformed choice are same as for spherical. Here, the potentials namely BW 91, CW 76 and Prox 77 perform appropriately below the barrier and Bass 80 seems to be good option above the barrier while Prox 88 overestimates the data.

The results of the fusion excitation function in the heavy mass region for the reaction $^{64}\text{Ni} + ^{130}\text{Te}$ are shown in Fig. 3.5(c). In this case the results are similar to spherical choice. Here Bass 80, Prox 77 and BW 91 estimates the cross section better in comparison to other potentials, while Prox 88 and CW 76 perform badly.

For the reaction $^{35}\text{Cl} + ^{238}\text{U}$ in the super-heavy mass region, the results are shown in Fig. 3.5(d). With the inclusion of deformation and orientation, the calculated fusion cross section overestimates as compared to experimental data. In this mass region, the fusion cross sections for the reaction $^{35}\text{Cl} + ^{238}\text{U}$ are consistent with the result of reaction $^{27}\text{Al} + ^{238}\text{U}$ of Set-I. Here, Prox 77 shows better agreement with the experimental data.

Out of all the calculations for two mentioned set of reactions, we have observed that in lighter mass region, with the spherical choice of nuclei, the behavior of different proximity potentials is similar for both the sets. The three potentials namely Bass 80, CW 76 and BW 91 perform comparatively better in relevance to experimental data.

After including the effect of deformation and orientation, it is observed that the performance of potentials doesn't change. With inclusion of deformation and orientation, cross section is increased. In the intermediate mass region, for the spherical choice Bass 80 best fits the experimental data while after including the deformation effect, Prox 77 holds well. After moving towards the heavier mass region, Bass 80 expresses the fair behavior for spherical as well as for deformed choice of nuclei. At last, in super heavy mass region, we examined that Bass 80 holds good result in spherical case while after the inclusion of deformation and orientation, Prox 77 behaves better in comparison to other potentials.

References:-

- [1]. J. Randrup and J. S. Vaagen, Phys. Lett. B **77**, 170 (1978).
- [2]. J.R. Birkelund and J. R. Huizenga, Phys. Rev. C **17**, 126 (1978).
- [3]. I. Dutt and R. K. Puri, Phys. Rev. C **81**, 064609 (2010); *ibid* 81, 064608, 2010.
- [4]. C. Y. Wong, Phys. Rev. Lett. **31**, 766 (1973).
- [5]. R. Kumar, M. K. Sharma, and R. K. Gupta, Nucl. Phys. A **870**, 42(2011).
- [6]. G. Montagnoli *et.al.*, Phys. Rev. C **90**, 044608 (2014).
- [7]. M. Beckerman, M.K. Salomaa, J. Wiggins and R. Rohe , Phys. Rev. C **28**, 1963 (1983).
- [8]. Tapan Rajbongshi *et.al.*, Phys. Rev. C **93**, 054622 (2016).
- [9]. W. Q. Shen *et.al.*, Phys. Rev. C **36**, 115 (1987).
- [10]. Z. Kohley, Phys. Rev. A **457**, 441 (1986).
- [11]. R. J. Charity, J. R. Leigh , J. J. M. Bokhorst , A. Chatterjee , G. S. Foote , D. J. Hinde, J. O. Newton, S. Ogaza, D. Ward, Nucl. Phys. A **457**, 441 (1986).

Summary

In the present work, the role of different proximity potentials in estimating the fusion excitation functions for the various reactions chosen from different mass region of the periodic table has been studied using the Wong formula. This analysis has been carried out with spherical as well as for deformed choice of nuclei. It is observed that the deformation impart significant effect on barrier characteristics which results in modification of fusion cross section, especially in below barrier region. Different proximities provide information of nuclear structure effect in different mass regions. As a result, the performance of proximity potential changes as we move from lighter to super heavy mass region. In lighter mass region, Bass 80, BW 91 and CW 76 perform better in comparison to other potentials. The behavior of Bass 80 and Prox 77 is in decent in agreement with experimental data for intermediate mass region. In heavy mass region, Bass 80 and BW 91 performs nicely. On moving towards the super heavy mass region, we observed that Prox 77 and Bass 80 performs best. Hence, to obtain the fusion cross section in different mass region, a proper choice of proximity potential is required. Interestingly, it is observed that the Bass 80 potential is common for both the sets from different mass regions. However, at energies below the Coulomb barrier further investigations are required.

Different proximity potential which overestimates the experimental data could be further improved by using ℓ - summed Wong formula. In this work, we have tried to test the effectiveness of proximity potential by considering the two set of reactions from different mass regions of the Periodic table. In order to achieve an overall generalized choice of proximity potentials in different mass region further investigations on large number of target- projectile combinations are required.